Invited paper

OPTO-ELECTRONICS REVIEW **10**(4), 231–236 (2002)

Recent advances in gate dielectrics and polarised light emission from GaN

S.J. PEARTON[1], C.R. ABERNATHY[2], B.P. GILA[1], A.H. ONSTINE[1], M.E. OVERBERG[1], G.T. THALER[1], JIHYUN KIM[2], B. LUO[2], R. MEHANDRU[2], F. REN[2], and Y.D. PARK[3]

[1]Department of Materials Science and Engineering, University of Florida, Gainesville, FL 32611, USA
[2]Department of Chemical Engineering, University of Florida, Gainesville, FL 32611, USA
[3]Center for Strongly Correlated Materials Research, Seoul National University, Seoul, 151–747, Korea

Inversion behaviour has been demonstrated in gate-controlled p-GaN diodes using both MgO and Sc_2O_3 gate dielectrics and implanted n^+ regions to provide a source of inversion charge. The total surface state density was estimated from capacitance-voltage or charge pumping measurements to be in the range 3–8 $\times 10^{12}$ cm^{-2} after the implant activation annealing to form the source and drain regions. In addition, Mn doping of GaN during growth by molecular beam epitaxy is found to produce room temperature ferromagnetism under conditions where the material remains single-phase. The layers can be used as injectors of spin-polarised carriers into light-emitting diode structures, with the potential for creating polarised optical output.

Keywords: GaN, magnetic semiconductors, gate dielectrics.

1. Introduction

There is significant interest in developing gate dielectrics for GaN, which allow for metal-insulator-semiconductor (MIS) or metal-oxide-semiconductor (MOS) controlled transistors [1–13]. These would have numerous advantages over metal gate devices, including typically better thermal stability and lower gate leakage. A further advantage of MOS or MIS GaN-based transistors would be the possibility of also using the gate oxide/insulator material as a surface passivation film. Current state-of-the-art AlGaN/GaN HEMTs generally show a decrease in drain current at high drain-source voltage [14]. This collapse of the current produces a severe degradation of the rf output power. One of the main mechanisms for the phenomena is the presence of surface states in the region between the drain and source. The use of SiN_x passivation layers on top of the AlGaN/GaN structure helps to partially mitigate the current collapse [14].

We have also found that oxides such as Sc_2O_3 and MgO are effective in reducing the effect of surface states on AlGaN/GaN HEMTs and, in addition, exhibit promise as gate dielectrics in GaN [15–17]. In particular, the Sc_2O_3 produces more stable passivation of the GaN surface than MgO. The Sc_2O_3 had a bixbyite crystal structure, with a 9.2% lattice mismatch to GaN, a high dielectric constant (14) and reasonable bandgap (6.3 eV). In this letter we report on the capacitance-voltage (C-V) characteristics of gate-controlled Sc_2O_3/GaN diodes. The total number of surface states was estimated from the voltage shift of the C-V curves and found to be 8.2×10^{12} cm^{-2}.

The field of semiconductor spin transfer electronics (spintronics) seeks to exploit the spin of charge carriers in semiconductors. It is widely expected that new functionalities for electronics and photonics can be achieved if the injection, transfer and detection of carrier spin can be controlled above room temperature. Since the magnetic properties of ferromagnetic semiconductors are a function of carrier concentration in the material in many cases, then it will be possible to have electrically or optically-controlled magnetism through field-gating of transistor structures or optical excitation to alter the carrier density. The development of magnetic semiconductors with practical ordering temperatures could lead to new classes of device and circuits, including spin transistors, ultra-dense non-volatile semiconductor memory and optical emitters with polarised output. In this paper we will also detail the achievement of room temperature ferromagnetism in (Ga,Mn)N and its utilisation in light-emitting diode (LED) structures.

2. Experimental

The starting sample for the inversion experiments was a 1 μm thick p-GaN (hole concentration is ~2×10^{17} cm^{-3} at 25°C) layer grown on a 2 μm undoped GaN buffer grown on a Al_2O_3 substrate by metal organic chemical vapour deposition. The Sc_2O_3 was deposited by rf plasma-activated molecular beam epitaxy (MBE) at 650°C using elemental Sc evaporated from a standard effusion cell at 1130°C and

*e-mail: spear@mse.ulf.edu

O_2 derived from an electron cyclotron plasma source operating at 200 W forward power (2.45 GHz) and 10^{-4} Torr. More details of the oxide growth and pre-cleaning of the GaN surface have been given previously [15,16]. The Sc_2O_3 layers were ~400 Å thick. N^+ regions were created by selective implantation of Si^+ at multiple energies and doses (70 keV, 2×10^{13} cm^2, 195 keV, 6×10^{13} cm^{-2} and 380 keV, 1.8×10^{14} cm^{-2}). The junction depth was ~0.4 µm from ion range simulations. The samples were then annealed at 950°C under N_2 to activate the Si-implanted regions. Windows were etched into the oxide and e-beam deposited p-ohmic (Ni/Au), n-ohmic (Ti/Al/Pt/Au) and gate metal (Pt/Au) were patterned by lithography. The separation of the n^+ regions was ~60 µm.

3. Results and discussion

3.1. Gate-controlled diodes

A Sc_2O_3/p-GaN MOS diode without the n^+ regions to provide an external source of minority carriers cannot remain in thermal equilibrium as the applied gate bias is swept from negative to positive polarity because of the extremely low minority carrier generation rate in the wide bandgap (3.4 eV) GaN. Only deep-depletion characteristics were observed up to a measurement temperature of 300°C. Achievement of inversion was not possible due to the low concentration of thermally generated electrons.

Figure 1 shows the C-V_G characteristics for various biases on the n^+-p junction diode. There are several key features of the data. Firstly, clear inversion behaviour is observed as electrons supplied from the n^+ regions are drawn into the gate. Secondly, when the n^+-p junction is reversed-biased, the onset of inversion is delayed, as demonstrated by the threshold voltage shift apparent in the C-V curves. This is the classical behaviour experienced for a gate-controlled MOS diode [18]. Thirdly, the presence of a hook region in the C-V curve is caused by a surface-state-induced barrier against electron flow at the boundary of the MOS diode. This type of behaviour has been reported previously for both SiC [19] and SiC [20] gate-controlled diodes and results from the nonequilibrium characteristics of deep level surface traps on the semiconductor. The total concentration of surface states, N_{SS} can be obtained from the relation [21]

$$N_{SS} \sim (\Delta V C_0)/e$$

where ΔV is the voltage difference between the two minima in the characteristic obtained with a grounded n^+ region, C_0 is the Sc_2O_3 capacitance under the gate and e is the electronic charge. Future work will be able to establish the role of the implant activation anneal in this trap density for GaN MOS diodes.

Inversion was obtained at 25°C for a measurement frequency of 150 kHz, while the accumulation capacitance exhibits a strong dependence of frequency with roughly a factor of two differences when the frequency is decreased from 1 MHz to 150 kHz. To explain the frequency-dependence of capacitance data, we need to invoke the presence of an interfacial layer between the stoichiometric Sc_2O_3 and p-GaN that produces an impedance contribution. The resistance of the interfacial layer is assumed to decrease with frequency due to an increase in hopping conductance and this produces the observed decrease in accumulation capacitance with increasing measurement frequency [22]. Once again, we are investigating the effect of the implanted activation anneal on the resulting C-V characteristics and the extent of any interfacial layers.

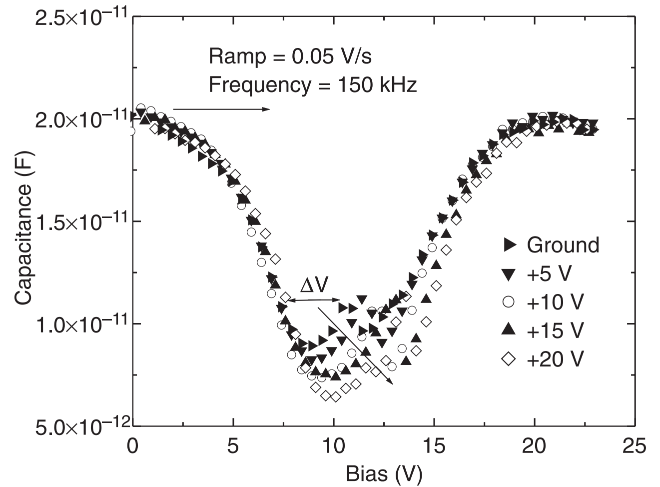

Fig. 1. C-V characteristics of Sc_2O_3/p-GaN gated diodes as a function of drain bias at 25°C in the dark. The voltage ramp rate was 0.05 Vs^{-1} and measurement frequency 150 kHz.

Figure 2 shows the measured charge-pumping current (I_{CP}) as a function of gate pulse frequency. The current increases linearly with this frequency beyond 100 Hz where leakage effects become negligible. The linear increase in I_{CP} at higher frequencies confirms the so-called charge-pumping action in which a fixed charge is measured for each gate pulse. This charge is injected across the n^+-p junctions in the gated diode. The surface-state density, N_{SS}, can be related to the pulse frequency and charge-pumping current I_{CP} through the relation

$$N_{SS} = \frac{I_{CP}}{\upsilon A_C e}$$

where A_C is the diode channel area and e is the electronic charge. From the frequency-dependence of the charge pumping current data, we obtain $N_{SS} = 3\times10^{12}$ cm^{-2} at the Sc_2O_3/p-GaN interface. This surface trap density is comparable to that reported previously for SiO_2/SiC gated diodes that had been prepared with a similar implantation process cycle [20]. Note that no effort has been made in our structures to passivate surface states through forming gas anneals or plasma hydrogenation. This is the first measure-

 © 2002 COSiW SEP, Warsaw

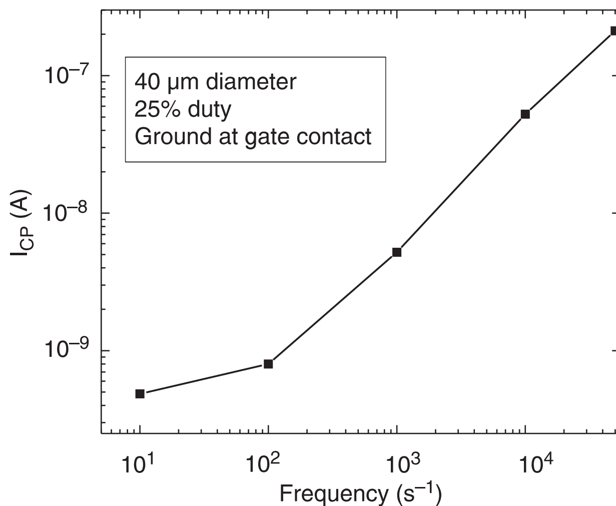

Fig. 2. Charge-pumping current vs. gate pulse frequency.

ment of surface state density in GaN-based MOS structures that more fully approximate a transistor, i.e., the structures show inversion and have gone through an extensive device processing sequence [23,24]. Note that we achieved similar results for MgO/p-GaN diodes [25,26].

3.2. Ferromagnetism in GaN and application to spin-LEDs

There are two major criteria for selecting the most promising materials for semiconductor spintronics. First, the ferromagnetism should be retained to practical temperatures (i.e. > 300 K). Second, it would be a major advantage if there were already an existing technology base for the material in other applications. Most of the work in the past has focused on (Ga,Mn)As and (In,Mn)As. However, the highest Curie temperatures reported for these materials (~110 K for (Ga,Mn)As [27] and ~35 for (In,Mn)As [28]) are too low for most practical applications.

The key breakthrough that focused attention on wide bandgap semiconductors as being the most promising for achieving practical ordering temperatures was the theoretical work of Dietl *et al*. [29]. They predicted that cubic GaN doped with ~5 at.% of Mn and containing a high concentration of holes (3.5×10^{20} cm^{-3}) should exhibit a Curie temperature exceeding room temperature.

Two basic approaches to understand the magnetic properties of dilute magnetic semiconductors have emerged. The first class of approaches is based on mean-field theory. The theories that fall into this general model implicitly assume that the dilute magnetic semiconductor (DMS) is a more-or-less random alloy, e.g., (Ga,Mn)N, in which Mn substitutes for one of the lattice constituents. The second class of approaches suggests that the magnetic atoms form small (a few atoms) clusters that produce the observed ferromagnetism [30]. A difficulty in experimentally verifying the mechanism responsible for the observed magnetic properties is that depending on the growth conditions employed for growing the DMS material. It is likely that one could readily produce samples that span the entire spectrum of possibilities from single-phase random alloys to nanoclusters of the magnetic atoms to precipitates and second phase formation. Therefore, it is necessary to decide on a case-by-case basis which mechanism is applicable.

The mean field approach basically assumes that the ferromagnetism occurs through interactions between the local moments of the Mn atoms, which are mediated by free holes in the material. The spin-spin coupling is also assumed to be a long-range interaction, allowing use of a mean-field approximation [31–36]. In its basic form, this model employs a virtual-crystal approximation to calculate the effective spin-density due to the Mn ion distribution. The direct Mn-Mn interactions are antiferromagnetic so that the Curie temperature, T_C, for a given material with a specific Mn concentration and hole density (derived from Mn acceptors and/or intentional shallow level acceptor doping), is determined by a competition between the ferromagnetic and anti-ferromagnetic interactions.

Initial reports of the energy level of Mn in GaN show it is very deep in the gap, E_V + 1.4 eV [37], and thus would be an ineffective dopant under most conditions. Some strategies for enhancing the hole concentration do exist, such as co-doping both acceptors and donors to reduce self-compensation effects [38] or the use of selectively-doped AlGaN/GaN superlattices in which there is transfer of free holes from Mg acceptors in the AlGaN barriers to the GaN quantum wells.

A further issue that needs additional exploration in the theories is the role of electrons, rather than holes, in stabilising the ferromagnetism in DMS materials. All of the reports of ferromagnetism in (Ga,Mn)N, for example, occur for material that is actually n-type. Since the material has to be grown at relatively low temperatures to avoid Mn precipitation and therefore only MBE can be used, there is always the possibility of unintentional n-type doping from nitrogen vacancies, residual lattice defects or impurities such as oxygen. Therefore stoichiometry effects, crystal defects or unintentional impurities may control the final conductivity, rather than Mn or the intentionally-introduced acceptor dopants.

While most of the theoretical work for DMS materials has focused on the use of Mn as the magnetic dopant, there has been some progress on identifying other transition metal atoms that may be effective. The predicted stability of ferromagnetic states in GaN doped with different 3d transition metal atoms found that (Ga,V)N and (Ga,Cr)N showed stable ferromagnetism for all transition metal concentrations whereas Fe, Co or Ni doping produced spin-glass ground states [39]. For the case of Mn, the ferromagnetic state was the lowest energy state for concentrations up to ~20%, whereas the spin-glass state became the most stable at higher Mn concentrations.

In epitaxial GaN layers grown on sapphire substrates and then subjected to solid state diffusion of Mn at temperatures from 250–800°C for various periods, clear signa-

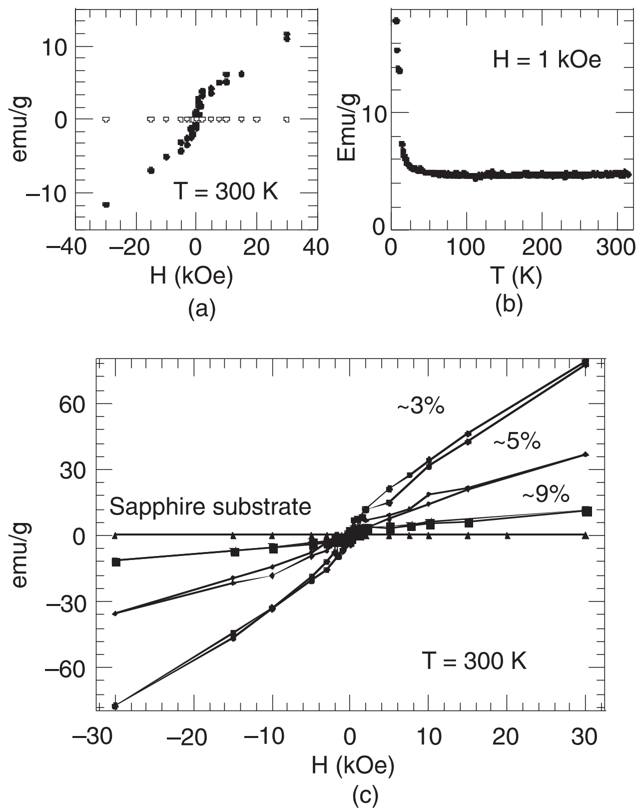

Fig. 3. (a) B-H at 300 K from MBE-grown (Ga,Mn)N with ~9 at. % Mn (closed circles). The data from the sapphire substrate is shown as open circles. (b) Magnetisation as a function of temperature for the MBE-grown (Ga,Mn)N with ~9 at. % Mn. (c) B-H at 300 K from MBE-grown (Ga,Mn)N with various Mn concentrations.

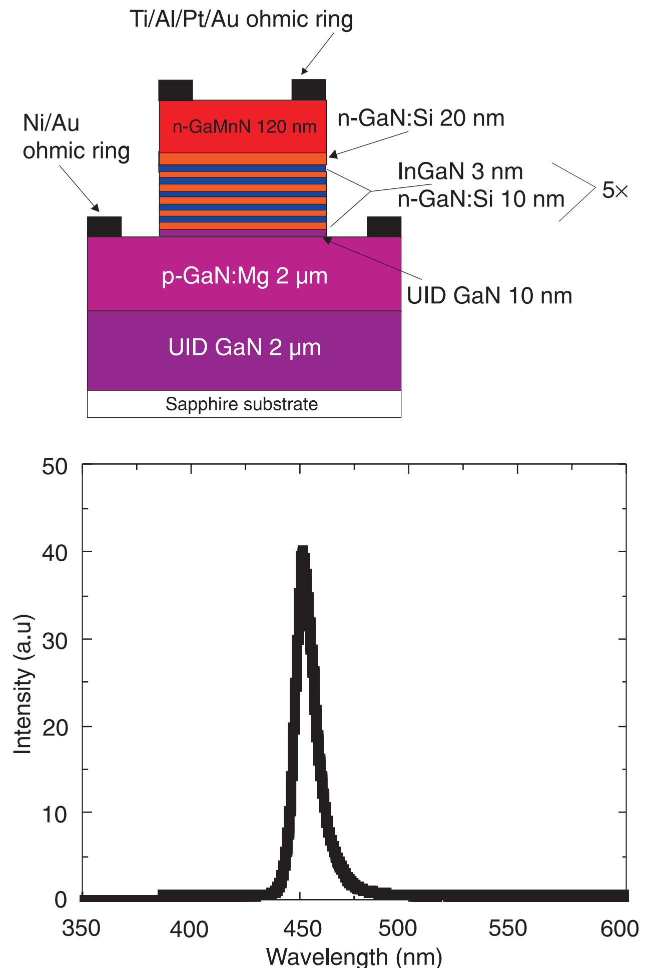

Fig. 4. (Ga,Mn)N/InGaN/GaN light-emitting diode structure (top) and spectral output from the device (bottom).

tures of room temperature ferromagnetism were observed [40,41]. The Curie temperature was found to be in the range 220–370 K, depending on the diffusion conditions. The use of ion implantation to introduce the Mn produced lower magnetic ordering temperatures [42].

In (Ga,Mn)N films grown by MBE at temperatures between 580–720°C with Mn contents of 6–9 at.%, magnetisation (M) versus magnetic field (H) curves showed clear hysteresis at 300 K, with coercivities of 52–85 Oe and residual magnetisations of 0.08–0.77 emu/g at this temperature [43]. The temperature dependence of the magnetisation for a sample with 9 at. % Mn, yielded an estimated T_C of 940 K using a mean field approximation. Note that while the electrical properties of the samples were not measured, they were almost certainly n-type. Room temperature ferromagnetism in n-type (Ga,Mn)N grown by MBE has also been reported by Thaler *et al.* [44]. Figure 3 shows M-T and M-H data as a function of Mn content in the GaMnN. In that case, strenuous efforts were made to exclude any possible contribution from the sample holder in the superconducting quantum interference device (SQUID) magnetometer or other spurious effects. It is also worthwhile to point out that for the studies of (Ga,Mn)N showing ferromagnetic ordering by magnetisation measurements, a number of materials characterisation techniques did not show the presence of any second ferromagnetic phases within detectable limits. In addition, the values of the measured coercivities are relatively small. Figure 4 (top) shows a spin-LED structure, in which the top n-contact layer is ferromagnetic GaMnN. When bias is applied to the device, it operates as an efficient blue LED (bottom). We are currently determining the temperature dependence of the spin injection efficiency in these structures.

Acknowledgements

The work at UF is partially supported by ONR (H.B. Dietrich, N00014-1-02-04) and NSF(DMR0101438 and CTS 9901173). The work at SNU was partially supported by KOSEF and Samsung Electronics Endowment through CSCMR.

References

1. F. Ren, M. Hong, S.N.G. Chu, M.A. Marcus, M.J. Schurman, A. Baca, S.J. Pearton, and C.R. Abernathy, “Ef-

 © 2002 COSiW SEP, Warsaw

fect of temperature on $GdGa_2O_3$ /GaN MOSFETS", *Appl. Phys. Lett.* **73**, 3893–3895 (1998).
2. M. Asif Khan, X. Hu, A. Tarakji, G. Simin, J. Yang, R. Gaska, and M.S. Shur, "AlGaN/GaN MOS heterostructure FETs on SiC substrates", *Appl. Phys. Lett.* **77**, 1339–1341 (2001).
3. G. Simin, X. Hu, N. Ilinskaya, J. Zhang, A. Tarakji, A. Kumar, J. Yang, M. Asif Khan, R. Gaska, M.S. Shur, "Large periphery high power AlGaN/GaN MOS heterostructure FETs on SiC with oxide bridging", *IEEE Electron. Dev. Lett.* **22**, 53–55 (2001).
4. B.P. Gaffey, L.J. Guido, X.W. Wang, and T.P. Ma, "High quality oxide/nitride/oxide gate insulator for GaN MIS structures", *IEEE Trans. Electron Dev.* **ED48**, 458–463 (2001).
5. S.C. Binari, K. Doverspike, G. Kelner, H.B. Dietrich, and A.E. Wickenden, "Fabrication and characterisation of GaN FETs", *Solid-State Electron.* **41**, 177–182 (1997).
6. S. Arulkumaran, T. Egawa, H. Ishikawa, T. Jimbo, and M. Umeno, "Investigations of SiO_2/n-GaN and SiN/GaN insulator interfaces with low interface state density", *Appl. Phys. Lett.* **73**, 809 (1998).
7. Y. Irokawa and Y. Nakano, "Observation of inversion behaviour in n-GaN planar MIS capacitor", *Solid-State Electron.* **46**, 1559–1564 (2002).
8. T.S. Lay, M. Hong, J. Kwo, J.P. Mannaerts, W.H. Hung, and D.J. Huang, "Energy band parameters at the GaAs and GaN Ga_2O_3 interfaces", *Solid-State Electron.* **45**, 1679–1683 (2001).
9. T. Hashizume, E. Alekseev, D. Pavlidis, K.S. Boutros, and J. Redwing, "C-V characterisation of AlN/GaN MIS structures grown on sapphire by MOCVD", *J. Appl. Phys.* **88**, 1983–1987 (2000).
10. N.Q. Zhang, S. Keller, G. Parish, S. Heikman, S.P. DenBaars, and U.K. Mishra, "High breakdown GaN HEMT with overlapping gate structure", *IEEE Electron Device Lett.* **21**, 421–423 (2000).
11. R. Therrien, G. Lucovsky, and R.F. Davis, "MIS structures on GaN", *Phys. Stat. Solidi.* **A176**, 793–796 (1999).
12. J.W. Johnson, B.P. Gila, B. Luo, K.P. Lee, C.R. Abernathy, S.J. Pearton, J.I. Chyi, T.E. Nee, C.M. Lee, C.C. Chou, and F.Ren, "SiO_2 /GdO/GaN MOSFETS", *J. Electrochem. Soc.* G303–306 (2001).
13. J.W. Johnson, B. Luo, F. Ren, B.P. Gila, V. Krishnamoorthy, C.R. Abernathy, S.J. Pearton, J.I. Chyi, T.E. Nee, C.M. Lee, and C.C. Chuo, "GdO/GaN MOSFET", *Appl. Phys. Lett.* **77**, 3230–3232 (2000).
14. S.C. Binari, K. Ikossi, J.A. Roussos, W. Kruppa, D. Park, H.B. Dietrich, D.D. Koleske, A.E. Wickenden, and R.L. Henry, "Trapping effects and microwave power performance in AlGaN/GaN HEMTs", *IEEE Trans. Electron Dev.* **48**, 465–471 (2001).
15. B.P. Gila, J.W. Johnson, R. Mehandru, B. Luo, A.H. Onstine, K.K. Allums, V. Krishnamoorthy, S. Bates, C.R. Abernathy, F. Ren and S.J. Pearton, "Gadolinium oxide and scandium oxide: gate dielectrics for GaN MOSFETs", *Phys. Stat. Solidi* **A188**, 239–242 (2001).
16. B. Luo, J.W. Johnson, J. Kim, R.M. Mehandru, F. Ren, B.P. Gila, A.H. Onstine, C.R. Abernathy, S.J. Pearton, A.G. Baca, R.D. Briggs, R.J. Shul, C. Monier, and J. Han, "Influence of MgO passivation on AlGaN/GaN HEMTs", *Appl. Phys. Lett.* **80**, 1661–1663 (2002).
17. B. Luo, J.W. Johnson, B.P. Gila, A.H. Onstine, C.R. Abernathy, F. Ren, S.J. Pearton, A.G. Baca, A.M. Dabiran, A.M. Wowchack, and P.P. Chow, "Surface passivation of AlGaN/GaN HEMTs using MBE-grown MgO or Sc_2O_3", *Solid-State Electron.* **46**, 467–475 (2002).
18. D.K. Schroder, *Advanced MOS Diodes*, Addison Wesley Longman, NY, 1986.
19. A. Goetzberger and J.C. Irvin, "Low temperature hysteresis effects in MOS Si capacitors caused by surface-state trapping", *IEEE Trans. Electron Dev.* **ED15**, 1005–1009 (1968).
20. S.T. Sheppard, J.A. Cooper, Jr., and M.R. Melloch, "Non-equilibrium characteristics of the gate-controlled diode in 6H-SiC", *J. Appl. Phys.* **75**, 3205–3207 (1994).
21. S. Grove and D.J. Fitzgerald, "Measurement of interface state density in MOS structures", *Solid-State Electron.* **9**, 783–786 (1966).
22. J. Jiang, O.O. Awadelkarim, D.O Lee, P. Roman, and J. Ruzyllo, "On the capacitance of metal/high-k dielectric material stack/Si structures", *Solid-State Electron.* (in press)
23. R. Mehandru, B.P.Gila, J.Kim, J.W. Johnson, K.P. Lee, B. Luo, A.H. Onstine, C.R. Abernathy, S.J. Pearton, and F. Ren, "Electrical characterisation of GaN MOS diode using Sc_2O_3 as the gate oxide", *Electrochem. Solid-State Lett.* **5**, G51–54 (2002).
24. J. Kim, R. Mehandru, B. Luo, F. Ren, B.P. Gila, A.H. Onstine, C.R. Abernathy, S.J. Pearton, and Y. Irokawa, "Characteristics of MgO/GaN gate controlled MOS diodes", *Appl. Phys. Lett.* **81**, 373–375 (2002).
25. J. Kim, R. Mehandru, B. Luo, F. Ren, B.P. Gila, A.H. Onstine, C.R. Abernathy, S.J. Pearton, and Y. Irokawa, "Inversion behaviour in Sc_2O_3/GaN gated diodes", *Appl. Phys. Lett.* **80**, 4555–4557 (2002).
26. J. Kim, B. Gila, R. Mehandru, J.W. Johnson, J.H. Shin, K.P. Lee, B. Luo, A. Onstine, C.R. Abernathy, S.J. Pearton, and F. Ren, "Electrical characterisation of GaN MOS diodes using MgO as the gate dielectric", *J. Electrochem. Soc.* **149**, G482–484 (2002).
27. H. Ohno, D. Chiba, F. Matsukura, T. Omiya, E. Abe, T. Dietl, Y. Ohno, and K. Ohtani, "Electric field control of ferromagnetism", *Nature* **408**, 944–946 (2000).
28. H. Ohno, F. Matsukura, and Y. Ohno, "Semiconductor spin electronics", *JSAP International* **5**, 4–9 (2002).
29. T. Dietl, H. Ohno, F. Matsukura, J. Cibert, and D. Ferrand, "Zener model description of ferromagnetism in magnetic zinc-blende semiconductor", *Science* **287**, 1019–1022 (2000).
30. M. Van Schilfgaarde and O.N. Myrasov, "Anomalous exchange interactions in III-V dilute magnetic semiconductors", *Phys. Rev.* **B63**, 233205–233209 (2001).
31. T. Dietl, H. Ohno, and F. Matsukura, "Hole-mediated ferromagnetism in tetrahedrally coordinated semiconductors", *Phys. Rev.* **B63**, 195205–195209 (2001).
32. T. Jungwirth, W.A. Atkinson, B.H. Lee, and A.H. MacDonald, "Interlayer coupling in ferromagnetic semiconductor superlattices", *Phys. Rev.* **B59**, 9818–9823 (1999).
33. M. Berciu and R.N. Bhatt, "Effects of disorder on ferromagnetism in diluted magnetic semiconductors", *Phys. Rev. Lett.* **87**, 108203–108206 (2001).
34. R.N. Bhatt, M. Berciu, M.D. Kennett, and X.J. Wan, "Diluted magnetic semiconductors in the low carrier density regime", *J. Superconductivity: Incorporating Novel Magnetism* **15**, 71–75 (2002).

35. V.I. Litvinov and V.K. Dugaev, "Ferromagnetism in magnetically doped III-V semiconductors", *Phys. Rev. Lett.* **86**, 5593–5596 (2001).
36. J. Konig, H.H. Lin, and A.H. MacDonald, "Theory of diluted magnetic semiconductor ferromagnetism", *Phys. Rev. Lett.* **84**, 5628–5631 (2001).
37. R.Y. Korotkov, J.M. Gregie, and B.W. Wessels, "Optical properties of the deep Mn acceptor in GaN:Mn", *Appl. Phys. Lett.* **80**, 1731–1733 (2002).
38. H. Katayama-Yoshida, R. Kato, and T. Yamamoto, "New valence control and spin control method in GaN and AlN by co-doping and transition atom doping", *J. Cryst. Growth* **231**, 438–442 (2001).
39. K. Sato and H. Katayama-Yoshida, "Material design of GaN-based ferromagnetic diluted magnetic semiconductors", *Jap. J. Appl. Phys.* **40**, L485–487 (2001).
40. M.L. Reed, M.K. Ritums, H.H. Stadelmaier, M.J. Reed, C.A. Parker, S.M. Bedair, and N.A. El-Masry, "GaMnN-a new material for spintronics", *Mater. Lett.* **51**, 500–502 (2001).
41. M.L. Reed, N.A. El-Masry, H.H. Stadelmaier, M.E. Ritums, N.J. Reed, C.A. Parker, J.C. Roberts and S.M. Bedair, "Room temperature ferromagnetic properties of (Ga,Mn)N", *Appl. Phys. Lett.* **79**, 3473–3475 (2001).
42. N.A. Theodoropoulou, A.F. Hebard, M.E. Overberg, C.R. Abernathy, S.J. Pearton, S.N.G. Chu, and R.G. Wilson, "Magnetic and structural properties of Mn-implanted GaN", *Appl. Phys. Lett.* **78**, 3475–3477 (2001).
43. S. Sonoda, S. Shimizu, T. Sasaki, Y. Yamamoto, and H. Hori, "MBE of wurtzite (Ga,Mn)N films on sapphire (0001) showing ferromagnetic behaviour at room temperature", *J. Cryst. Growth* **237–239**, 1358–1364 (2002).
44. G.T. Thaler, M.E. Overberg, B. Gila, R. Frazier, C.R. Abernathy, S.J. Pearton, J.S. Lee, S.Y. Lee, Y.D. Park, Z.G. Khim, J. Kim and F. Ren, "Magnetic properties of n-GaMnN thin films", *Appl. Phys. Lett.* **80**, 3964–3966 (2002).

 © 2002 COSiW SEP, Warsaw